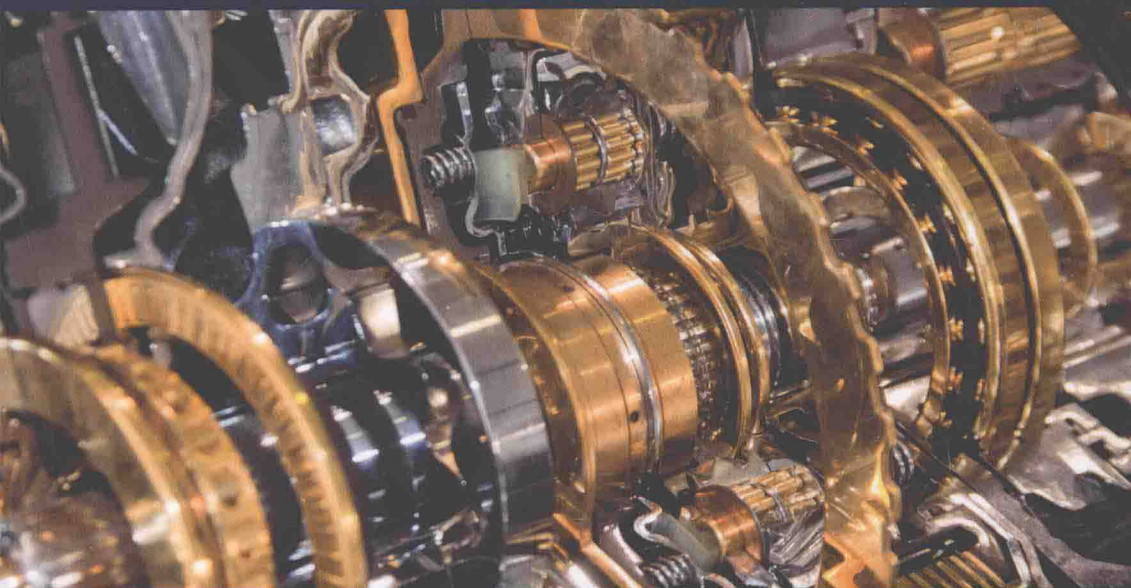


NUMERICAL METHODS IN ENGINEERING SERIES



Internal Combustion Engine Bearings Lubrication in Hydrodynamic Bearings

**Dominique Bonneau
Aurelian Fatu
Dominique Souchet**

ISTE

WILEY

Series Editor
Piotr Breitkopf

Internal Combustion Engine Bearings Lubrication in Hydrodynamic Bearings

Dominique Bonneau
Aurelian Fatu
Dominique Souchet

ISTE

WILEY

First published 2014 in Great Britain and the United States by ISTE Ltd and John Wiley & Sons, Inc.

Apart from any fair dealing for the purposes of research or private study, or criticism or review, as permitted under the Copyright, Designs and Patents Act 1988, this publication may only be reproduced, stored or transmitted, in any form or by any means, with the prior permission in writing of the publishers, or in the case of reprographic reproduction in accordance with the terms and licenses issued by the CLA. Enquiries concerning reproduction outside these terms should be sent to the publishers at the undermentioned address:

ISTE Ltd
27-37 St George's Road
London SW19 4EU
UK

www.iste.co.uk

John Wiley & Sons, Inc.
111 River Street
Hoboken, NJ 07030
USA

www.wiley.com

© ISTE Ltd 2014

The rights of Dominique Bonneau, Aurelian Fatu and Dominique Souchet to be identified as the authors of this work have been asserted by them in accordance with the Copyright, Designs and Patents Act 1988.

Library of Congress Control Number: 2014942902

British Library Cataloguing-in-Publication Data

A CIP record for this book is available from the British Library

ISBN 978-1-84821-684-6



Printed and bound in Great Britain by CPI Group (UK) Ltd., Croydon, Surrey CR0 4YY

Preface

This volume is the fourth and final part of the series devoted to hydrodynamic bearings.

Volume 1 [BON 14a] describes in detail the lubricant physical properties that play an essential role in hydrodynamic phenomena, followed by hydrodynamic lubrication equations and models for their numerical solutions. Part of Volume 1 also gives “elastohydrodynamic” (EHD) model descriptions.

Volume 2 [BON 14b] is devoted to the study of mixed lubrication. The role of surface roughness is analyzed using the corresponding numerical techniques both from a hydrodynamic and a surface asperity contact point of view. This volume also addresses the issue of surface wear in the aforementioned context.

Volume 3 [BON 14c] describes several thermohydrodynamic (THD) models and thermoelastohydrodynamic (TEHD) problems. This volume ends with a description of general algorithms used in computational software designed to describe bearings under large non-stationary loads.

This last volume (Volume 4) addresses specific problems related to engine and compressor bearing calculations.

Chapter 1 of this volume describes the kinematic and dynamic relationships of the mobile part (crank shaft, connecting rod, piston) of an internal combustion engine.

Chapters 2, 3 and 4 are devoted to different system bearings, respectively, connecting rod big and small end bearings and crank shaft journal bearings. The specific problems associated with each one are analyzed in detail: lubricant supply,

multibody rods and bearings with coupled operation, etc. Several examples specific to different types of combustion engines are illustrated in these three chapters.

Chapter 5 describes practical bearing calculation techniques for optimizing lubrication conditions. A reliable, simple and easy approach for optimizing multiple objects, based on methods used in experimental design, is used to create mathematical models for optimizing chosen parameter values, e.g. in the case of engine bearings: power loss and criteria for severity evaluation. These models are later used in the optimization phase to replace complicated numerical simulations used for calculating bearing lubrication parameters.

An application to internal combustion engine connecting rod big end bearing calculations is described in detail.

Bibliography

- [BON 14a] BONNEAU D., FATU A., SOUCHET D., *Hydrodynamic Bearings*, ISTE, London and John Wiley & Sons, New York, 2014
- [BON 14b] BONNEAU D., FATU A., SOUCHET D., *Mixed Lubrication in Hydrodynamic Bearings*, ISTE, London and John Wiley & Sons, New York, 2014
- [BON 14c] BONNEAU D., FATU A., SOUCHET D., *Thermo-hydrodynamic Lubrication in Hydrodynamic Bearings*, ISTE, London and John Wiley & Sons, New York, 2014

Nomenclature

Points, basis, repairs, links and domains

A	point at the junction crank shaft – connecting rod (2D model)
B	point at the junction connecting rod – piston (2D model)
O	origin point of lubricant film repair (developed bearing)
O_c	origin point of the repair attached to the housing (bearing center)
O_a	origin point of the repair attached to the shaft
$\mathbf{x}, \mathbf{y}, \mathbf{z}$	Cartesian basis for the film (developed bearing)
$\mathbf{x}_c, \mathbf{y}_c, \mathbf{z}_c$	Cartesian basis for the housing
B_i	$\{\mathbf{x}_i, \mathbf{y}_i, \mathbf{z}_0\}$, basis of the repair \mathfrak{R}_i
\mathfrak{R}_0	$\{O, \mathbf{x}_0, \mathbf{y}_0, \mathbf{z}_0\}$, engine block repair
\mathfrak{R}_1	$\{O, \mathbf{x}_1, \mathbf{y}_1, \mathbf{z}_0\}$, crank shaft repair
\mathfrak{R}_2	$\{A, \mathbf{x}_2, \mathbf{y}_2, \mathbf{z}_0\}$, connecting rod repair
\mathfrak{R}_3	$\{O, \mathbf{x}_3, \mathbf{y}_3, \mathbf{z}_0\}$, small end shaft repair
\mathfrak{R}_4	$\{O, \mathbf{x}_4, \mathbf{y}_4, \mathbf{z}_0\}$, piston repair
L_{ij}	link between the solid S_i and the solid S_j

Scalars

B	m	bearing half-width
C	m	bearing radial clearance
C_p	$\text{J kg}^{-1} \text{ } ^\circ\text{C}^{-1}$	specific heat
D	Pa; m	universal variable representing p else $r - h$
E	N m^{-2}	Young modulus
F_N, F_T	N	normal and tangential contact force components

H	$\text{W m}^{-2} \text{ } ^\circ\text{C}^{-1}$	thermal transfer coefficient
I_i	kg m^2	central moment of inertia for solid S_i with respect to O z axis
K_N, K_T	N m^{-1}	penalization stiffness for a contact problem
L	m	bearing width
L_b	m	connecting rod length
M_{xc}	N m	\mathbf{x}_c component for the moment at O_c of $\mathfrak{S}_{pressure}$ torsor
M_{yc}	N m	\mathbf{y}_c component for the moment at O_c of $\mathfrak{S}_{pressure}$ torsor
R	m	bearing radius
R_v	m	crank shaft radius
S	m^2	piston surface
U	m s^{-1}	shaft peripheral velocity for a bearing
V	m s^{-1}	squeeze velocity for a bearing
W	m s^{-1}	shaft axial velocity for a bearing
W_{xc}	N	\mathbf{x}_c component of $\mathfrak{S}_{pressure}$ torsor resultant
W_{yc}	N	\mathbf{y}_c component of $\mathfrak{S}_{pressure}$ torsor resultant
d	m	distance between the piston shaft and the crank shaft center (2D model)
f		Coulomb friction coefficient
h	m	lubricant film thickness
k		relative position of the con rod mass center with respect to the big end axis
k	$\text{W m}^{-1} \text{ } ^\circ\text{C}^{-1}$	thermal conductivity
m_i	kg	mass of solid S_i
p	Pa	pressure in the lubricant film
p_{supply}	Pa	supply pressure for a bearing
p_g	Pa	combustion gas pressure acting on the piston
t	s	time
u	m s^{-1}	circumferential velocity component at a point into the film
u_N, u_T	m	normal and tangential displacements at a contact point
v	m s^{-1}	velocity squeeze component at a point into the film
w	m s^{-1}	axial velocity component at a point into the film
x	m	circumferential coordinate for a point into the film
y	m	coordinate in the thickness direction for a point into the film
z	m	axial coordinate for a point into the film
α	$^\circ\text{Pa}^{-1}$	piezoviscosity coefficient

β	$^{\circ}\text{C}^{-1}$	thermoviscosity coefficient
$\varepsilon_x, \varepsilon_y$		relative eccentricity components
ζ_x, ζ_y	rad	misalignment components for the shaft into the housing
θ	rad	angular coordinate for a film point for a bearing
θ_y	rad	crank shaft angle
μ	Pa.s	lubricant dynamic viscosity
ρ	kg m^{-3}	lubricant density
σ	m	combined roughness of film walls
φ	rad	connecting rod angle with respect to the engine block
χ	rad	con rod small end axis angle with respect to the engine block
ψ	rad	connecting rod angle with respect to the crank shaft
ω	rad s^{-1}	shaft angular velocity with respect to the housing

Dimensioned parameters

\bar{R}	R_y/L_h
\bar{d}	d/L_h
\bar{h}	h/σ

Torsors

$\mathfrak{S}_{\text{pressure}}$	pressure actions exerted on the housing
$\mathfrak{S}_{\text{applied load}}$	loading for a shaft or thrust bearing

Matrices

$[A]$	N Pa^{-1}	integration matrix
$[C]$	m Pa^{-1}	compliance matrix
$[K]$	N m^{-1}	stiffness matrix
$[A_i]$		matrix of the problem i equation discretized by the finite element method
$[J]$		Jacobian matrix

Indices

<i>F</i>	film or lubricant
<i>S</i>	shaft, solid
<i>supply</i>	lubricant supply
<i>amb</i>	ambient medium

Acronyms

BDC	bottom dead center
CPV	contact pressure velocity product
DOE	design of experiments
EA	evolutionary algorithm
EHD	elastohydrodynamic
GT	global thermal (method)
MFT, MOFT	minimum (oil) film thickness
MOFP	maximum oil film pressure
MTM	mean temperature method
PTM	parabolic temperature profile method
SAE	Society of Automotive Engineers
TDC	top dead center
TEHD	thermoelastohydrodynamic

Contents

PREFACE	ix
NOMENCLATURE	xi
CHAPTER 1. KINEMATICS AND DYNAMICS OF CRANK SHAFT–CONNECTING ROD–PISTON LINKAGE	1
1.1. Kinematic model of crank shaft–connecting rod–piston linkage.	2
1.1.1. Model description	2
1.1.2. Expressions of angular velocities	5
1.1.3. Expressions of velocity for points A , G_2 and B	5
1.1.4. Expressions of connecting rod angular acceleration and points G_2 and B accelerations.	7
1.2. Efforts in the links between the crank shaft, the connecting rod and the piston	8
1.2.1. Hypothesis and data.	8
1.2.2. Dynamics equations for the piston.	9
1.2.3. Dynamics equations for the axis	9
1.2.4. Dynamics equations for the connecting rod.	10
1.2.5. Dynamics equations for the crank shaft	11
1.2.6. Efforts for frictionless links	12
1.3. Load diagram correction in the case of large deformations.	13
1.3.1. Kinematics of crank shaft–connecting rod–piston system with mobility	14
1.3.2. Dynamics of crank shaft–connecting rod–piston system with mobility	20

1.4. Examples of link efforts between the elements of crank shaft-connecting rod-piston system	23
1.4.1. Data	23
1.4.2. Load diagrams for the connecting rod big end bearing	24
1.4.3. Load diagrams for a connecting rod small end bearing	26
1.4.4. Load diagrams for a crank shaft main bearing	27
1.4.5. Engine torque	28
1.5. Bibliography	29
CHAPTER 2. THE CRANK SHAFT-CONNECTING ROD LINK	31
2.1. Geometrical and mechanical characteristics of the connecting rod big end bearing.	31
2.2. Lubricant supply	33
2.3. Correction of the load diagram in the case of large deformations.	34
2.4. Multibody models	38
2.4.1. Interfaces and interactions: main assumptions	39
2.4.2. Equations of unilateral contact with friction and equilibrium equations	41
2.4.3. Compliance matrices	42
2.4.4. Finite element modeling of the contact in the joint plane	46
2.4.5. Modelization of the contact between the housing and the shells	65
2.5. Case of V engines	72
2.6. Examples of connecting rod big end bearing computations.	79
2.6.1. Presentation of connecting rods and corresponding load diagrams	80
2.6.2. Geometry and lubricant data	84
2.6.3. Analysis of some isothermal results	85
2.6.4. Influence of mesh downsizing	96
2.6.5. Search of potential damage zones due to cavitation	98
2.6.6. Examples taking into consideration thermoelastohydrodynamic effects	100
2.7. Bibliography	118

CHAPTER 3. THE CONNECTING ROD–PISTON LINK	123
3.1. Geometrical particularities and mechanics of connecting rod–piston link	123
3.2. Lubricant supply	125
3.3. Example of computation for a connecting rod small end bearing with the axis embedded into the piston.	127
3.4. Complete model of the connecting rod–piston link	133
3.4.1. Equations.	134
3.4.2. Integration of dynamics equation	137
3.4.3. Piston structural model	139
3.4.4. Example: the piston–axis–connecting rod small end link for a Formula 1 engine	142
3.5. Bibliography	158
CHAPTER 4. THE ENGINE BLOCK–CRANK SHAFT LINK	161
4.1. Geometrical and mechanical particularities of the engine block – crank shaft link	161
4.2. Lubricant supply	162
4.3. Calculus of an isolated crank shaft bearing	163
4.4. Complete model of the engine block – crank shaft link.	170
4.4.1. Model presentation	171
4.4.2. Expression of the elastic deformations	173
4.4.3. Expression of the film thickness	175
4.4.4. Equation system	175
4.4.5. Resolution method	178
4.4.6. Examples.	180
4.5. Bibliography	196
CHAPTER 5. INFLUENCE OF INPUT PARAMETERS AND OPTIMIZATION	197
5.1. Design of experiments method	197
5.2. Identification of the input parameters: example	201
5.3. Multiobjective optimization.	202
5.4. Optimization of a connecting rod big end bearing: example	204
5.4.1. Viscosity factors.	208
5.4.2. Radial clearance factor	209
5.4.3. Radial shape defect	209
5.4.4. Axial shape defect.	210
5.4.5. Shell bore relief factors	210

5.4.6. Supply pressure and temperature.	210
5.4.7. Power loss	211
5.4.8. Contact pressure velocity factor	211
5.4.9. Severity criterion based on the minimum film thickness	212
5.4.10. Leakage	213
5.4.11. Global functioning temperature.	214
5.4.12. Bearing optimization method	214
5.5. Bibliography	221
INDEX	223

Kinematics and Dynamics of Crank Shaft–Connecting Rod–Piston Linkage

In an internal combustion engine, the combination of mechanical parts, which allows the force exerted by the combustion of gas to be transformed into rotational movement resulting in vehicle wheel rotation, is referred to as “the moving part”. This includes pistons, piston pins, connecting rod bearings, connecting rods and the crank shaft. The small elements related to sealing or assembling the piston and lock rings for piston pin positioning are not discussed. Because of their low mass, these connecting elements barely influence the forces created by the moving part. The connecting rod consists of a set of assembled solid objects: connecting rod beam, cap, bearings, screws, washers and possibly nuts. It will be assumed that there is no movement between these various elements of the connecting rod.

The aim of this chapter is to determine the kinematic relationships between elements of the moving part and forces involved in the junctions. Although these elements are made up of elastic materials and are thus capable of deformation under the effect of force transmission, in this chapter they will be considered non-deformable.

The junctions between the elements of the moving part are generally made with sliding bearings. These require a lubricant film layer in order to function well. The extra hundredths of a millimeter occupied by the layer contribute to the general junction mobility and additional mobility of very small amplitudes. This notable extra mobility significantly complicates the kinematic model of the moving part.

A study on dynamics using a complete kinematic model requires knowledge of junction static and dynamic properties, e.g. all the coefficients of stiffness and damping matrices of each link, the dimensions of each matrix is equal to the degrees of freedom. The developments and examples presented in other chapters of this

book show that the elastohydrodynamic behaviors of lubricated bearings in non-stationary conditions are such that they make it impossible to construct a dynamic model where the bearings would be represented by stiffness and damping matrices known in advance. Once again, the purpose of this chapter is to give the necessary background needed for junction forces calculations. A kinematic and dynamic model where the junctions are reduced to their core mobility is sufficient for acquiring results with the desired precision. In section 1.3, a model is developed that takes into account the extra mobility added by the significant deformability of the connecting rod bearing.

1.1. Kinematic model of crank shaft–connecting rod–piston linkage

1.1.1. Model description

The moving part examined is assumed to be those of a single-cylinder engine made up of five non-deformable bodies numbered from 0 to 4 as follows:

- 0: engine block;
- 1: the crank shaft with the center of rotation O and the center of mass G_1 ;
- 2: the connecting rod AB with the center of mass G_2 ;
- 3: the element coupling the connecting rod and the piston;
- 4: the piston.

The mechanism plan consists of a closed kinematic chain located in a Cartesian plane $O(x_0, y_0)$. Only the basic mobility of the junctions between these solid bodies will be considered as follows:

- L_{01} : pivoting link between the engine block and the crank shaft with the center O and axis Oz_0 ;
- L_{12} : pivoting link between the crank shaft and the connecting rod with the center A and axis Az_0 ;
- L_{23} : sliding pivoting link between the connecting rod and the axis with the center B and axis Bz_0 ;
- L_{34} : pivoting link between the piston pin and the piston with the center B and axis Bz_0 ;

– L_{04} : annular linear link¹ between the engine block and the piston with the center O and axis D \mathbf{x}_0 .

Figure 1.1 shows the kinematic diagram of this model. In this figure, we can see the basis and the parameters used. To simplify notation, the basis vectors use the same notations as the frame axis. For example, the frame \mathcal{R}_0 of the engine block has O as the point of origin and axis $O\mathbf{x}_0$, $O\mathbf{y}_0$ and $O\mathbf{z}_0$. The base of this frame consists of orthonormal vectors \mathbf{x}_0 , \mathbf{y}_0 and \mathbf{z}_0 . Because of this similarity, the vector notation is not shown in the figure.

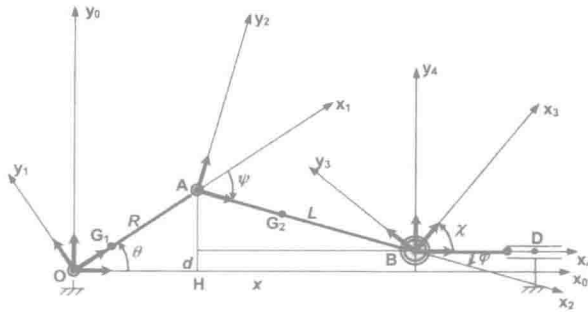


Figure 1.1. Kinematic model

The reference frames and basis are defined as follows:

- $\mathcal{R}_0 \equiv \{O, \mathbf{x}_0, \mathbf{y}_0, \mathbf{z}_0\}$: engine block frame;
- $\mathcal{R}_1 \equiv \{O, \mathbf{x}_1, \mathbf{y}_1, \mathbf{z}_0\}$: crank shaft frame;
- $\mathcal{R}_2 \equiv \{A, \mathbf{x}_2, \mathbf{y}_2, \mathbf{z}_0\}$: connecting rod frame;
- $\mathcal{R}_3 \equiv \{B, \mathbf{x}_3, \mathbf{y}_3, \mathbf{z}_0\}$: small end shaft frame;
- $\mathcal{R}_4 \equiv \{B, \mathbf{x}_4, \mathbf{y}_4, \mathbf{z}_0\} \equiv \{B, \mathbf{x}_0, \mathbf{y}_0, \mathbf{z}_0\}$: piston frame;
- $B_i \equiv \{\mathbf{x}_i, \mathbf{y}_i, \mathbf{z}_0\}$: basis of the frame \mathcal{R}_i .

The geometrical values used are as follows:

- R : the radius of the crank shaft;
- a : distance from center O to the crank shaft's center of mass G_2 ;
- L : connecting rod length;
- $k = AG_2/L$: position relative to point G_2 of the connecting rod;

¹ This choice is necessary for achieving a non-hyperstatic assembly.

– d : default alignment between the cylinder axis and the center of the crank shaft.

The parameters used are as follows:

- θ : crank shaft angle ($\mathbf{x}_0, \mathbf{x}_1$) relative to the engine block;
- ψ : connecting rod angle ($\mathbf{x}_1, \mathbf{x}_2$) with respect to the crank shaft;
- φ : connecting rod angle ($\mathbf{x}_0, \mathbf{x}_2$) with respect to the engine block;
- χ : connecting rod small end axis angle ($\mathbf{x}_0, \mathbf{x}_3$) with respect to the engine block;
- x : piston pin position with respect to the center of the crank shaft .

Except for the angle χ of the piston axis that is independent, these parameters are geometrically interrelated to one another as follows:

$$HA = R \sin \theta = d - L \sin \varphi$$

$$x = R \cos \theta + L \cos \varphi$$

$$\varphi = \theta + \psi$$

Knowing that $\bar{R} = \frac{R}{L}$ and $\bar{d} = \frac{d}{L}$, the following equations can be derived:

$$\sin \varphi = \bar{d} - \bar{R} \sin \theta \quad [1.1]$$

$$\cos \varphi = \sqrt{1 - (\bar{d} - \bar{R} \sin \theta)^2} \quad [1.2]$$

$$\varphi = \text{Arcsin}(\bar{d} - \bar{R} \sin \theta) \quad [1.3]$$

$$x = L \left(\frac{R}{L} \cos \theta + \cos \varphi \right) = L \left[\bar{R} \cos \theta + \sqrt{1 - (\bar{d} - \bar{R} \sin \theta)^2} \right] \quad [1.4]$$

for which only the independent parameters θ and χ are absolutely necessary.